

Structural Characterization of Doped GaSb Single Crystals by X-ray Topography

M.G. HÖNNICKE,^{1,5} I. MAZZARO,² J. MANICA,³ E. BENINE,²
E.M. DA COSTA,⁴ B.A. DEDAVID,⁴ C. CUSATIS,² and X.R. HUANG¹

1.—NSLS II, Brookhaven National Laboratory, Upton, NY, USA. 2.—LORXI, Departamento de Física, Universidade Federal do Paraná, Curitiba, PR, Brazil. 3.—Departamento de Engenharia Mecânica, Universidade Federal do Paraná, Curitiba, PR, Brazil. 4.—Departamento de Engenharia Mecânica e Mecatrônica, PUC-RS, Porto Alegre, RS, Brazil. 5.—e-mail: mhonnicke@bnl.gov

We characterized GaSb single crystals containing different dopants (Al, Cd, and Te), grown by the Czochralski method, using x-ray topography and high-angular-resolution x-ray diffraction. Lang topography revealed dislocations parallel and perpendicular to the crystal surface. Double-crystal GaSb 333 x-ray topography showed dislocations and vertical stripes that could be associated with circular growth bands. We compared our high-angular-resolution x-ray diffraction measurements (rocking curves) with findings predicted by the dynamical theory of x-ray diffraction. These measurements show that our GaSb single crystals have a relative variation in the lattice parameter ($\Delta d/d$) on the order of 10^{-5} . This means that they can be used as electronic devices (e.g., detectors) and as x-ray monochromators.

Key words: X-ray imaging, x-ray topography, Lang topography, double-crystal topography

INTRODUCTION

GaSb single crystals are group III–V semiconductors. They possess suitable properties for electronic devices (viz. transistors, detectors, infrared sources, and high-efficiency thermo-photovoltaic cells) especially due to their high electron mobility and small bandgap (~0.82 eV).^{1,2} Furthermore, the combination of band offsets and lattice matching with other semiconductor materials makes GaSb very valuable as a substrate for different electronic devices that are based on epitaxial thin films.

This manuscript has been authored by employees of Brookhaven Science Associates, LLC under Contract No. DE-AC02-98CH10886 with the U.S. Department of Energy. The publisher by accepting the manuscript for publication acknowledges that the United States Government retains a non-exclusive, paid-up, irrevocable, world-wide license to publish or reproduce the published form of this manuscript, or allow others to do so, for United States Government purposes. This preprint is intended for publication in a journal or proceedings. Since changes may be made before publication, it may not be cited or reproduced without the author's permission.

(Received September 15, 2009; accepted February 23, 2010;
published online March 23, 2010)

However, defects that can be present in its crystalline structure reduce electron mobility and can introduce stress/strain, and even defects, in the epitaxial film. The Czochralski technique is usually employed to grow GaSb crystals.^{1,3–7} Imperfections are expected (e.g., swirls, inclusions, and dislocations) during growth and will affect the crystal structure and its electronic properties. Intrinsic GaSb single crystals are always *p*-type. Dopants such as Al and Cd retain its *p*-type conductivity, while Te at concentrations over 10^{17} atoms/cm³ changes its conductivity to *n*-type. The advantage of Al and Cd dopants is that they reduce antisite defects.⁸

X-ray topography⁹ is a technique well suited to study structural defects in single crystals; it is sensitive to variations in the lattice parameter ($\Delta d/d$) because it is based on x-ray diffraction imaging of a single crystal. Variant techniques are reported in the literature: Berg-Barrett, Lang, and double-crystal topography (or plane-wave topography). More recently, synchrotron-based x-ray topography techniques (white-beam topography

and monochromatic-beam topography) have been widely used.^{10–14} The differences between these approaches are their sensitivity to $\Delta d/d$ and the type of defect detected.

High-angular-resolution x-ray diffraction is a complementary measurement method that can help to determine crystal quality. Such measurements are taken by fine angular rotation of the crystal around the diffraction condition, so-called rocking-curve measurement. These assessments can be made using conventional x-ray sources or synchrotron sources. Different setups are employed for rocking-curve measurements:¹⁵ (a) a dispersive setup using a four-crystal monochromator (conventional sources)¹⁶ or a monochromatic beam of a synchrotron source; and (b) a highly sensitive nondispersive setup based on high diffraction order.

In the present work, we used Lang topography, x-ray double-crystal topography, and rocking-curve measurements to characterize GaSb single crystals with different dopants [Al (*p*-type), Cd and Te (*n*-type)], grown by liquid-encapsulated Czochralski (LEC) in the [111] direction. We evaluated the quality of those crystals in relation to their practical application as electronic devices and x-ray monochromators, and discuss our findings herein.

EXPERIMENTAL PROCEDURES

Thin (300 μm) and thick (2 mm) crystals from GaSb ingots were oriented, cut, polished, and etched for analysis by Lang topography, double-crystal topography, and rocking-curve measurements. Four samples were used: (a) two (samples 1 and 2) oriented and cut in the [111] direction (300 μm thick, both Al doped at 10^{17} atoms/cm³), and (b) two (samples 3 and 4) oriented and cut in the [110] direction (2 mm thick, one Cd doped at 10^{17} atoms/cm³ and the other Te doped at 10^{18} atoms/cm³). All were etched (HF:HNO₃:CH₃COOH, 1:20:1) for 1 min three times, to remove the damaged layer due to cutting and polishing.

Lang topography, in the horizontal scattering plane, was carried out using a conventional x-ray source (long fine focus Mo target) (Fig. 1a). The x-ray tube was set in the line focus geometry, so that the source's horizontal width was 40 μm (for a takeoff angle of 6°) and vertically it was 12 mm long. A 1.1-m-long collimator with a 150- μm slit allowed us to select, by crystal diffraction, the energy of Mo K_{α1} (17.48 keV). The crystal was mounted on a Lang camera based on elastic translation.^{17,18} The images were acquired with high-spatial-resolution Kodak Industrex M5 film.

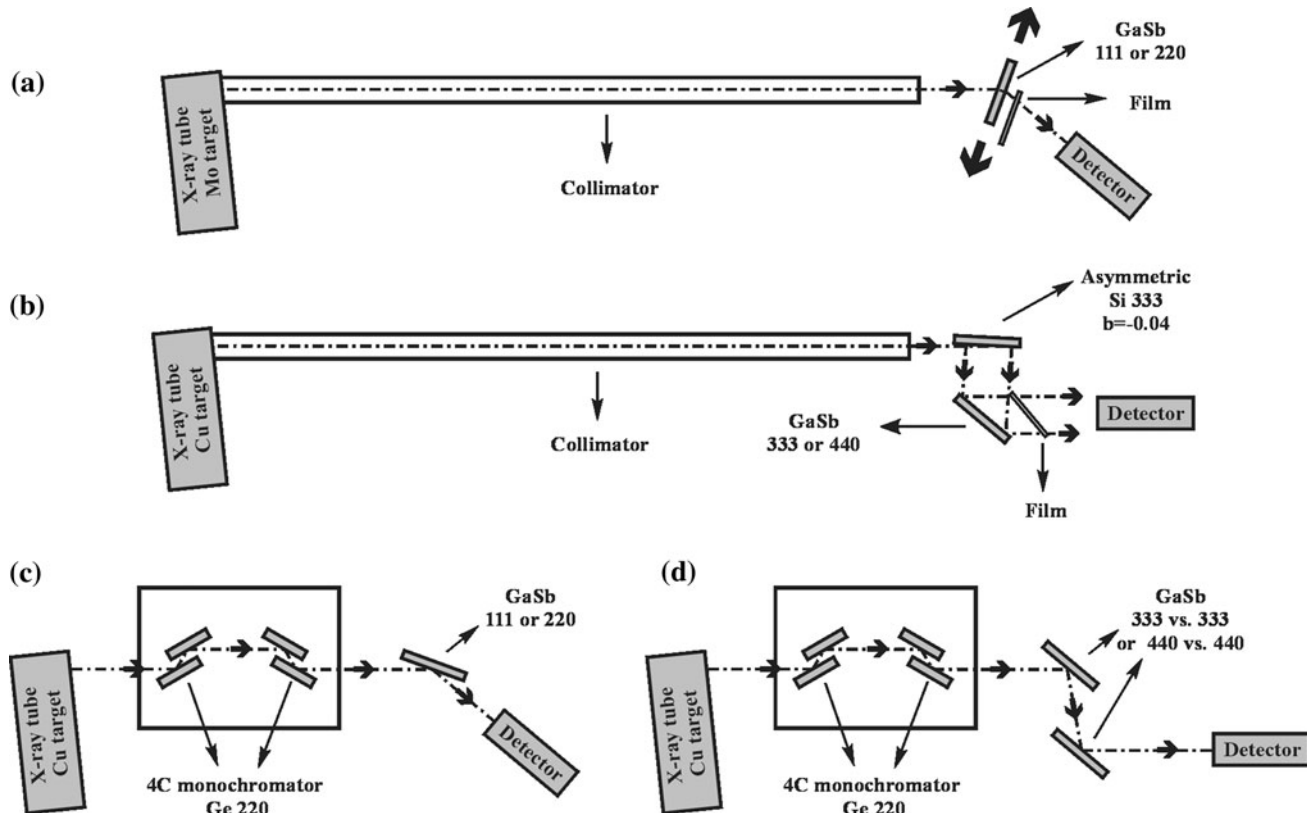


Fig. 1. Experimental setups for structural characterization of GaSb single crystals: (a) Lang topography (transmission geometry—Laue case); (b) double-crystal topography; (c) high-resolution x-ray diffraction based on four-crystal Ge 220 monochromator; and (d) ultrahigh-resolution x-ray diffraction for high-order reflections.

We also carried out high-resolution double-crystal x-ray topography (Fig. 1b) to better characterize these crystals. The x-ray tube (long fine focus) also was set in the line focus geometry. We employed the same 1.1-m-long collimator, but with a slit of 0.5 mm. As the first crystal, we employed an asymmetrically cut Si 333 monochromator (floating zone, $b = -0.04$; magnification $m = 25$) at 8.05 keV ($\text{Cu K}_{\alpha 1}$). The second crystal was the GaSb single crystal in different orientations of [111] and [110]. The images again were acquired with high-spatial-resolution Kodak Industrex M5 film.

Rocking-curve measurements were taken with two different setups. For low-order reflections (111 and 220), a Ge 220 four-crystal monochromator was employed (Fig. 1c) at 8.05 keV. For high-order reflections (333 and 440) we chose an ultrahigh-resolution nondispersing setup, more sensitive to $\Delta d/d$ (Fig. 1d), also at 8.05 keV.

X-RAY TOPOGRAPHY AND ROCKING-CURVE MEASUREMENTS

The Lang topography (Fig. 2a) was obtained from the thin GaSb 111 single crystals (samples 1 and 2, initially a single piece); however, for the 220 diffraction on transmission geometry (Laue case, Fig. 1a) at 17.48 keV. The resulting image shows several lines and small spots that, respectively, could reflect dislocations parallel or almost parallel to the surface, and normal or almost normal to the surface. The features resembling “holes” in the image might be dislocations or even other defects such as precipitates. However, most of the spots and stripes are diffuse, an appearance that could be caused by insufficient etching during removal of the disturbed layer, or even the vertical divergence of the current setup that might blur the image. More comprehensive studies are needed to clarify the origins of this effect.

To better characterize the sample, we undertook double-crystal x-ray topography (Fig. 1b) on the selected dashed area of Fig. 2a, at 8.05 keV for the GaSb 333 diffraction in reflection geometry (Bragg case). Such topography (Fig. 2b) does not show images of dislocations or any other defects in the crystal bulk. However, it is strongly sensitive to weak deformations near the crystal surface. Dislocations, precipitates, or even structures caused by insufficient etching when removing the disturbed layer are apparent in the image as large dark areas. Also, the image displays narrow vertical stripes that can be associated with circular growth bands. Double-crystal topography of samples 3 and 4 (Cd doped and Te doped, respectively) taken with 440 diffraction (not shown here) did not show such striations. Their absence might be due to the different orientation of the crystal, since all were grown under the same conditions (pulling velocity 5.2 mm/h, seed rotation 5 rpm). The striations almost always appear in GaSb crystals grown in the [111] direction via the Czochralski technique.

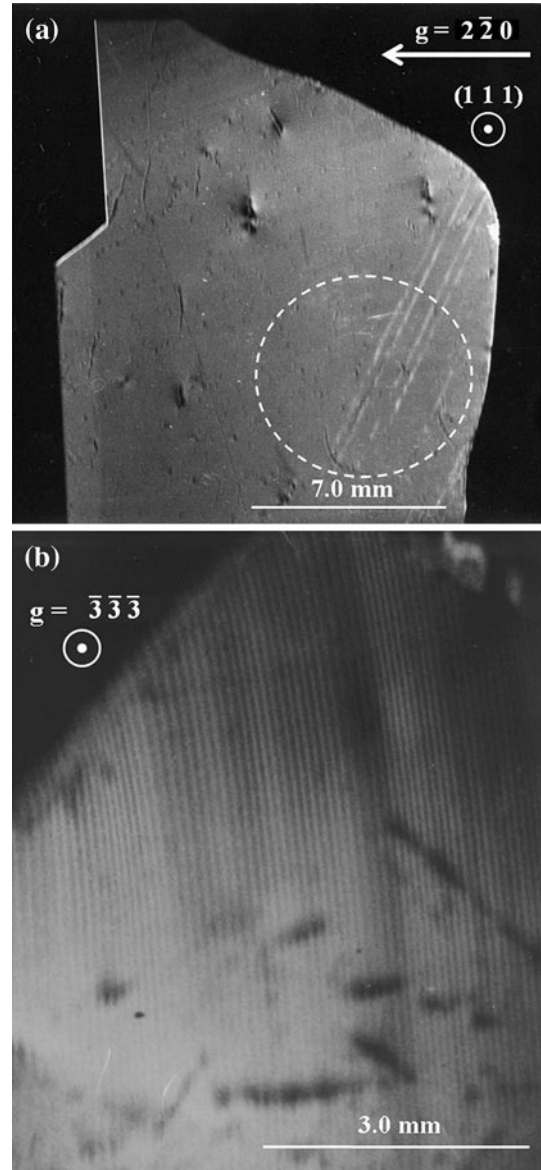


Fig. 2. (a) Lang topography (transmission geometry) of a 300- μm -thick GaSb 220 single crystal (Al doped); long fine focus Mo $\text{K}_{\alpha 1}$ (40 kV \times 20 mA), exposure time 30 h. (b) Double-crystal topography of the dashed area of the GaSb 333 single crystal shown in (a); long fine focus Cu $\text{K}_{\alpha 1}$ (40 kV \times 20 mA), exposure time 6 h.

This occurs because the method encompasses a substantial nonstationary growth process due to intense convective flows, misalignment of the axis of crystal rotation with respect to the axis of the thermal symmetry, concentration overcooling, and other issues.⁷ Together, these factors cause fluctuations in growth rate that are responsible for variations in the crystal composition, entailing formation of growth striations.⁷ A solution for this is to try to regrow the crystal by the vertical Bridgman method.⁷

We can consider the topography shown in Fig. 2b as plane-wave x-ray topography due to the experimental setup described in the “Experimental

Procedure" section. Accordingly, we can extract a $\Delta d/d$ map from the image. To obtain this map, we acquired the topography on the maximum slope at the high-angle side of the rocking curve. By considering the rocking curve of the GaSb 333 single crystal as a Gaussian profile with the same full-width of half-maximum (FWHM) as the diffraction curve predicted by the dynamical theory of x-ray diffraction (FWHM = 19.7 μrad), we can employ the following expression to determine the angular deviation ($\Delta\theta$) of the different points (a pixel-by-pixel approach) on the image:

$$\Delta\theta = \sigma \sqrt{\ln(I) + \ln(I_{\max})} + \omega, \quad (1)$$

where σ is the width of the Gaussian profile, I is the intensity at the different points in the image (pixels), I_{\max} is the maximum intensity of the image, and ω is the angular position on the rocking curve where the image was acquired. From the different

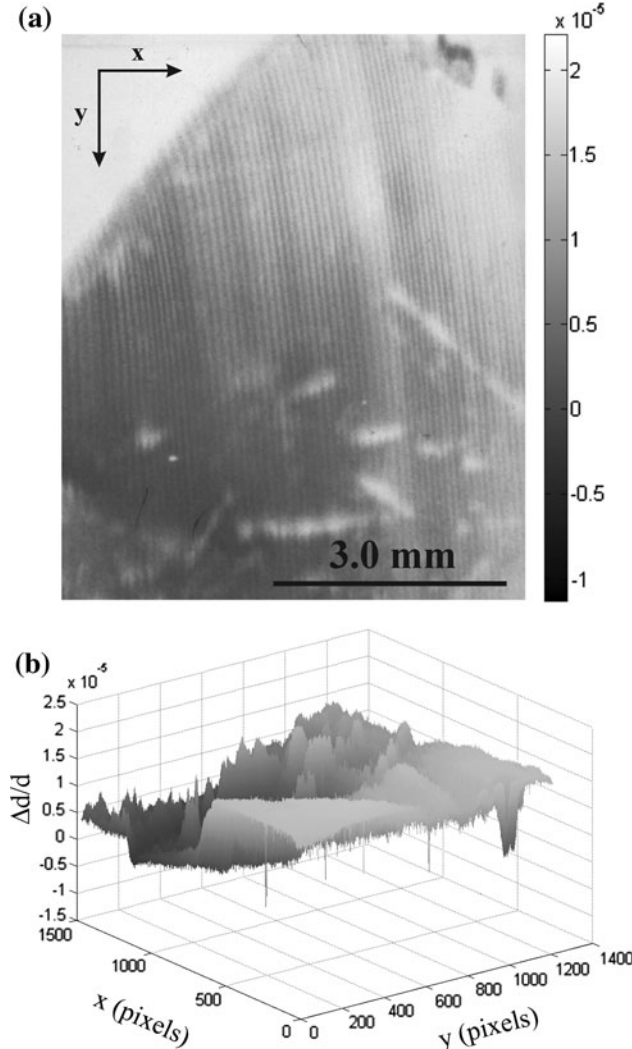


Fig. 3. (a) Two-dimensional map of the relative variations in the lattice parameter ($\Delta d/d$) based on the topography shown in Fig. 2b. (b) Three-dimensional map of the relative variations in the lattice parameter ($\Delta d/d$), also from the topography in Fig. 2b.

values for $\Delta\theta$ we can determine the relative variations in the lattice parameter ($\Delta d/d$):

$$\frac{\Delta d}{d} = -\cot(\theta)\Delta\theta, \quad (2)$$

where θ is the diffraction angle.

The two-dimensional (2D) and a three-dimensional (3D) map of $\Delta d/d$ is shown in Fig. 3a and b. Variations within $\Delta d/d \approx 10^{-5}$ are very apparent. The extinction depth (that is, the depth to which x-rays penetrate during diffraction)^{19–21} has values varying from 1 μm to 50 μm . So, the detected $\Delta d/d$, caused by dislocations, precipitates, or even structures due to insufficient etching, lies very close to the surface. Such variations were not detected by rocking-curve measurements; we did not identify any differences when comparing the experimental and the theoretical rocking curves [predicted by the dynamical theory of x-ray diffraction (Fig. 4)]. Also,

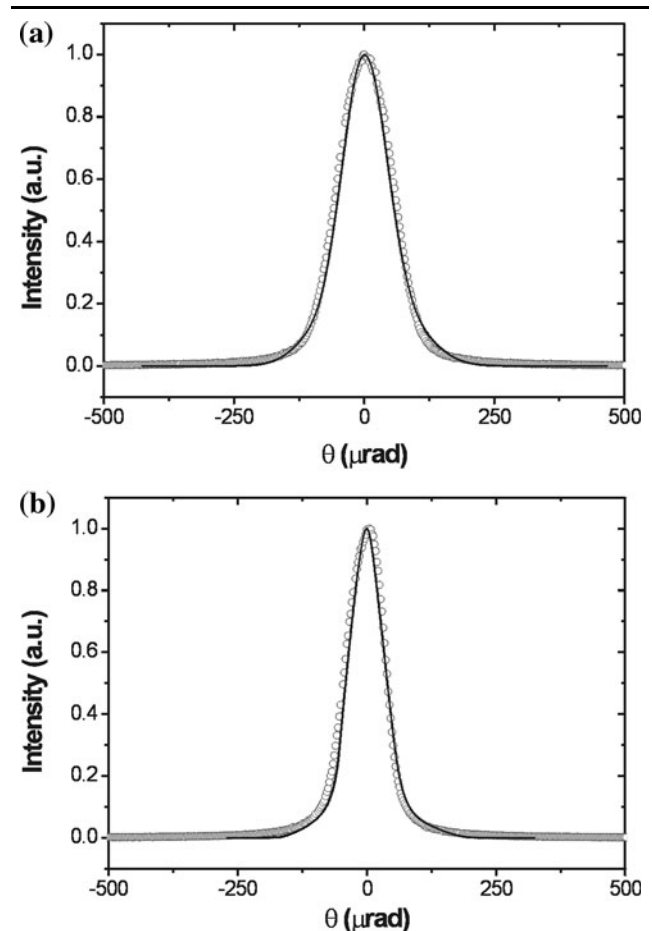


Fig. 4. (a) High-resolution x-ray diffraction measurement (rocking curve) on the GaSb 111 single crystal using the four-crystal Ge 220 monochromator (Fig. 1c). Solid line Theoretical rocking curve based on the dynamical theory of x-ray diffraction; open circles represent the experimental data. (b) Rocking-curve measurement on the GaSb 220 single crystal using the four-crystal Ge 220 monochromator (Fig. 1c). Solid line Theoretical rocking curve based on the dynamical theory of x-ray diffraction; open circles represent experimental data.

Table I. Full-width at half-maximum (FWHM) of rocking curves measured with the nondispersive setup (Fig. 1d)

Sample	Diffraction Plane	Experimental versus Theoretical FWHM (μrad)
1 × 2 (GaSb 111)	333	34 versus 30
3 × 4 (GaSb 110)	440	37 versus 37

high-order diffraction rocking-curve measurements (based on the nondispersive setup, more sensitive to $\Delta d/d$) showed no significant differences (Table I) for the FWHMs of the measured and theoretically predicted rocking curves. We anticipated both results. For the diffraction planes and the x-ray energy employed, the rocking-curve measurements are not sensitive to $\Delta d/d$ smaller than 10^{-5} , while topography is sensitive. This difference was already proven by several authors by strain mapping and $\Delta d/d$ mapping acquired with a rocking-curve imaging technique.^{13,14}

CONCLUSIONS

We characterized GaSb single crystals with different dopants grown by the liquid-encapsulated Czochralski technique via x-ray topography and high-resolution rocking curves.

Dislocations, precipitates, and growth bands were observed by different topographies. However, relative variations in the lattice parameter of about $\Delta d/d \approx 10^{-5}$ and the match between the measured and theoretically predicted rocking curves provide good reasons to try to use those crystals for electronic devices (detectors, for example, Te doped), and for x-ray monochromators (Al and Cd doped) in experiments that do not require high energy resolution. The crystal quality was found to be compatible with that of other GaSb single crystals reported in the literature. However, we were not able to detect that different dopants could help improve the crystal quality, as already described in the literature.¹ The detected growth striations can affect the electronic properties because, in these cases, the dislocation density can reach values of $10^2/\text{cm}^2$. For

non-high energy resolution monochromator applications this is not a serious problem. Finally, there were no significant variations between the measured and theoretically predicted rocking curves.

ACKNOWLEDGEMENTS

Part of this work was supported by the U.S. Department of Energy, Office of Science, Office of Basic Energy Sciences, under Contract No. DE-AC-02-98CD10886. The authors grateful acknowledge Avril Woodhead (BNL) for manuscript editing.

REFERENCES

1. E.M. Costa, B.A. Dedavid, and A. Muller, *Mater. Sci. Eng.* B44, 208 (1997).
2. A. Peles, A. Janotti, and C.G. Van de Walle, *Phys. Rev. B* 78, 035204 (2008).
3. J. Sestak, V. Sestakova, and B. Stepanek, *J. Therm. Anal. Calorim.* 56, 749 (1999).
4. J. Sestakova, B. Stepanek, and J. Sestak, *Cryst. Res. Technol.* 31, 929 (1996).
5. A.E. Voloshin, T. Nishinaga, P. Ge, and C. Huo, *J. Cryst. Growth* 234, 12 (2002).
6. A.E. Voloshin, T. Nishinaga, and P. Ge, *Crystallogr. Rep.* 47, S136 (2002).
7. I.A. Prokhorov, Yu.A. Serebryakov, B.G. Zakharov, I.Zh. Bezbakh, V.V. Ratnikov, and I.L. Shulpina, *J. Cryst. Growth* 310, 5477 (2008).
8. P.S. Dutta, H.L. Bhat, and V. Kumar, *Appl. Phys. Lett.* 81, 5821 (1997).
9. B.K. Tanner, *X-Ray Diffraction Topography* (Oxford: Pergamon, 1976).
10. A.N. Danilewsky, R. Simon, A. Fauler, M. Fiederle, and K.W. Benz, *Nucl. Instrum. Methods B* 199, 71 (2003).
11. M. Dudley, S.P. Wang, W. Huang, C.H. Carter, V.F. Tsvetkov, and C. Fazi, *J. Phys. D: Appl. Phys.* 28, A63 (1995).
12. R. Barrett, J. Baruchel, J. Hartwig, and F. Zontone, *J. Phys. D: Appl. Phys.* 28, A250 (1995).
13. D. Lubbert, C. Ferrari, P. Mikulik, P. Pernot, L. Helfen, N. Verdi, D. Korytar, and T. Baumbach, *J. Appl. Cryst.* 38, 91 (2005).
14. D. Lubbert, T. Baumbach, J. Hartwig, E. Boller, and E. Pernot, *Nucl. Instrum. Methods B* 160, 521 (2000).
15. J.W.M. DuMond, *Phys. Rev.* 52, 872 (1937).
16. S.E.G. Slusky and A.T. Macrander, *J. Appl. Cryst.* 20, 522 (1987).
17. J.E.A. Miltat (D. Phil. Thesis, University of Oxford, 1971).
18. M.G. Honnicke, I. Mazzaro, C. Cusatis, and V.H. Etgens, *Jpn. J. Appl. Phys.* 43, 5614 (2004).
19. A. Authier, *Dynamical Theory of X-ray Diffraction* (Oxford: Oxford University Press, 2001).
20. M.G. Honnicke and C. Cusatis, *J. Phys. D: Appl. Phys.* 38, A73 (2005).
21. M.G. Honnicke, C. Cusatis, and P.C. de Camargo, *J. Phys. D: Appl. Phys.* 41, 065401 (2008).